

Measurement of the Cross Section Asymmetry of the Reaction $\gamma p \rightarrow \pi^{\circ} p$ in the Resonance Energy Region $E_{\gamma} = 0.5 - 1.1$ GeV

F. V. Adamian, A. Yu. Buniatian, G. S. Frangulian*, P. I. Galumian[†], V. H. Grabski, A. V. Hairapetian, H. H. Hakopian, V. K. Hoktanian, J. V. Manukian, A. M. Sirunian, A. H. Vartapetian, H. H. Vartapetian, and V. G. Volchinsky
Yerevan Physics Institute, 2 Alikhanian Brothers St. Yerevan, 375036 Armenia

R. A. Arndt, I. I. Strakovsky, and R. L. Workman
*Center for Nuclear Studies and Department of Physics
The George Washington University, Washington, DC 20052, USA*
(November 10, 2018)

Abstract

The cross section asymmetry Σ has been measured for the photoproduction of π° -mesons off protons, using polarized photons in the energy range $E_{\gamma} = 0.5 - 1.1$ GeV. The CM angular coverage is $\theta_{\pi}^{*} = 85^{\circ} - 125^{\circ}$ with energy and angle steps of 25 MeV and 5° , respectively. The obtained Σ data, which cover the second and third resonance regions, are compared with existing experimental data and recent phenomenological analyses. The influence of these measurements on such analyses is also considered.

PACS numbers: 13.60.Le, 25.20.Lj

I. INTRODUCTION

Single-pion photoproduction has been used extensively to explore the electromagnetic properties of nucleon resonances, and most determinations of the $N\gamma$ resonance couplings [1] have been obtained through multipole analyses of this reaction. The study of N^{*} properties, in general, has enjoyed a resurgence, driven by the growth of new facilities worldwide. Many precise new measurements have focused on the photoproduction of pions and other pseudoscalar mesons, in the hope that they would reveal states not seen previously in the

*On leave from Yerevan Physics Institute

[†]On leave from Yerevan Physics Institute

photoproduction and elastic scattering of pions. Associated studies have suggested both new states and couplings to existing states which contradict those found in analyses of the full pion production database.

These results demonstrate the influence of measurements sensitive to new quantities and suggest that older analyses may have been based on insufficient or flawed data sets. A survey of existing data in the 1 GeV region shows most polarization measurements to have only one or two angular points at a given beam energy, often with rather large uncertainties. This allows a great deal of freedom in multipole analyses, and is clearly insufficient to pick out more than the strongest resonance signals.

One quantity which has consistently influenced these new analyses is the beam polarization quantity Σ . Examples include the E2/M1 ratio [2], where new measurements of the differential cross section and Σ changed this ratio by nearly a factor of two. Measurements of Σ in η photoproduction were shown [3,4] to be sensitive to the $A_{3/2}/A_{1/2}$ ratio of photo-decay amplitudes for the $D_{13}(1520)$, implying a ratio very different from the pion photoproduction value. The behavior of Σ in kaon photoproduction has also proved [5] to be crucial in determining the character of a bump seen in precise new total cross section measurements. In π^+n photoproduction, results for Σ from GRAAL have been used to argue for a change in the $A_{1/2}$ amplitude for the $S_{11}(1650)$ [6].

In this experiment, we have performed systematic measurements of the cross section asymmetry Σ for the reaction $\gamma p \rightarrow \pi^0 p$ [7] simultaneously with measurements of Compton scattering $\gamma p \rightarrow \gamma p$ [7,8], over the energy range $E_\gamma = 0.5 - 1.1$ GeV and at pion CM angles $\theta_\pi^* = 85^\circ - 125^\circ$. The experimental data (158 data points) from π^0 -meson photoproduction constitute the first systematic and high statistics measurement of Σ for this reaction channel over the present kinematic region. Preliminary results of the measurements have been presented in [9].

In Sections 2 and 3, we describe the methods employed in this experiment, with special emphasis on the control of systematic errors. In Section 4, we describe how these measurements, and the recent measurements from GRAAL [25], have effected the GW multipole analyses. Comparisons to the Mainz fits [10] are also made. Finally, in Section 5, we summarize our results.

II. EXPERIMENTAL SETUP

The experiment was carried out on the linearly polarized photon beam of the 4.5 GeV Yerevan Synchrotron. The same setup has been used for the parallel study of two reactions: Compton scattering and photoproduction of π^0 -meson off protons. The experimental setup is shown in Fig. 1.

The linearly polarized photon beam is generated by coherent bremsstrahlung (CB) of 3.0–3.5 GeV electrons on the internal 100 μm diamond crystal target. The beam has 2–3 msec long pulses with a 50 Hz repetition rate and an intensity of about 5×10^9 eq. photons/sec. The beam, shaped by a system of collimators and sweeping magnets, has a 10×10 mm size at the position (H_2) of the liquid hydrogen target (H_2) (9 cm in length). It is transported in a vacuum pipe to the Wilson-type quantameter (Q). The energy spectrum is measured and controlled by a 30-channel pair spectrometer PS-30 (energy resolution 1–2%) [11]. The whole range of bremsstrahlung energies are covered by 5 scans with respective current settings on

the PSM analyzing magnet. The full energy spectra of bremsstrahlung on amorphous and crystal targets, measured by the pair spectrometer PS-30, are presented in Fig. 2.

The recoil protons are detected by the magnetic spectrometer (MS) consisting of a doublet of quadrupole lenses (L_1, L_2), a bending magnet (BM), a telescope of four scintillation trigger counters ($S_1 - S_4$) and a system of coordinate detectors, including a scintillation hodoscope (H_p) and seven multiwire proportional chambers ($MWPC_{xy}$), allowing the reconstruction of momentum, azimuthal and polar angles of the outgoing proton. Time-of-flight measurements were carried out between S_1 and S_4 counters on a flight base of 9 m for particle identification (p, π). The MS covered a solid angle of $\Delta\Omega \approx 3.5 \text{ msr}$, and its angular and momentum resolutions were $\sigma_\theta \approx 0.3^\circ$, $\sigma_\phi \approx 0.2^\circ$ and $\sigma_P/P \approx 1\%$, respectively. The incident photon energy and the CM scattering angle were reconstructed on average with an accuracy of $\sigma_{E_\gamma}/E_\gamma \approx 1\%$ and $\sigma_{\theta^*} \approx 0.6^\circ$, with corresponding acceptances of $\approx 18\%$ and $\approx 7.5^\circ$, respectively.

The π^0 decay photons were detected by the Čerenkov spectrometer (\check{C}_s) consisting of a veto counter (V), a lead converter (Pb), scintillation hodoscope (H_{xy}) for x and y coordinate analysis, trigger counter (T), and a lead glass Čerenkov counter of full absorption (\check{C}). The energy resolution of the Čerenkov counter could be parameterized as $\sigma(E)/E = 0.08/\sqrt{E}$ without converter and $\sigma(E)/E = 0.1/\sqrt{E}$ with converter (E being the photon energy in GeV).

The kinematics of the analyzed process was completely determined by defining the kinematic parameters of the proton in the magnetic spectrometer. For identification of the process $\gamma p \rightarrow \pi^0 p$, the protons in the magnetic spectrometer were detected in coincidence with the photon detection branch. The coordinate detectors of the Čerenkov spectrometer were in addition used for correlation analysis between two detecting branches to identify the low rate yield of the Compton scattering process [7,8].

An independent experimental study was carried out to check the reconstruction accuracy in the magnetic spectrometer (MS) [7]. Monte Carlo calculations, intended to estimate the influence of different possible factors on the reconstruction precision, indicate that inaccuracies in setting the positions, angles and fields of magnetic elements, poor quality of track reconstruction in $MWPC_{xy}$, additional multiple scattering in materials not taken into account, influence equally the reconstruction accuracy of both the interaction vertex and the scattering angles in MS. Therefore, an experimental study of the vertex position reconstruction accuracy was defined as an effective test of the characteristics of the MS, and was easily carried out by means of a point-like target. Good agreement between the experimental results for vertex reconstruction and Monte Carlo calculations (Fig. 3) provides reliable support for the performance of our proton detection branch within designed precisions.

Finally, the possibility to treat Compton scattering data [7,8], despite significant difficulties caused by the physical background process of π^0 photoproduction with approximately two orders of magnitude higher cross section, and with practically the same kinematic parameters, also points to a reliable operation of the detection system within designed accuracies.

III. EXPERIMENT AND DATA ANALYSIS

During the measurements, several factors were considered to minimize the influence of systematic uncertainties. A particular emphasis has been placed on maintaining the stability

of the coherent peak position. In the case of its deviation, the event registration was paused, until respective correction procedure was made. Such checks of the coherent peak were carried out every 40–50 sec. In Fig. 4, the measured peak region is presented, superimposed on the full coherent bremsstrahlung spectrum, for the cases with correct and distorted peak position. A possible influence on the asymmetry results from instabilities in subsystems was compensated by periodical alternating the orientation of the photon beam polarization during the measurement of the same kinematic point. Also, during data acquisition the trigger rates, efficiencies of the coordinate detectors, distributions of kinematic variables were controlled. Hardware and software of all these control procedures was realized through the CAMAC standard. Fiber optic lines were used to manage the current of the pair spectrometer magnet (PSM) and the electronics of the MS trigger, placed immediately on the MS.

During the off-line analysis, prior to the reconstruction step, the time-of-flight measurements between S_1 and S_4 were analyzed, and the events with a proton candidate in MS were selected (Fig. 5). A soft cut was made, mainly at low energies, on the energy response of the Čerenkov detector, to reduce the contribution of accidental coincidences and multiparticle events resulting from the energetic part of the coherent bremsstrahlung spectrum [7]. Then, the selected events were sent for reconstruction of the kinematic parameters of proton and the kinematics of the event.

Within further selection, the interaction point in the target was reconstructed and events falling out of the target limits by more than one standard deviation are cut.

The yield of the $\gamma p \rightarrow \pi^0 p$ reaction was defined from the number of selected events in the time spectrum of start-stop measurements between two detection branches (Fig. 6), by fitting and subtracting the respective number of background events in the peak region.

Several corrections were applied to compensate for the contribution of various factors. The results from the analysis of Compton scattering process were used to correct for the influence of that source. Further corrections were applied, compensating for the rate reductions due to the dead time of data acquisition and efficiency of different subdetectors. The maximum trigger rates was about 5 event/sec, and the dead time did not exceed 10%. Another insignificant contribution, resulting from the empty target cell, was measured separately and amounted to $\sim 1\%$.

The background $p\gamma$ -rate is mainly dominated with double pion production processes generated by the high energy tail of CB spectrum. This background contribution has been determined in additional measurements, such as:

- $p\gamma$ -rate dependence on the coherent peak energy of the CB spectrum at fixed kinematics of the setup, allowing the significant variation in the relative yield of single and multiple pion production processes.
- The $p\gamma$ -rate dependence on the π^0 -photon decay angle.

The data obtained were then compared with results of Monte Carlo calculations. The contribution of background processes was estimated to be less than 5%.

Calculations of the polarization of the CB spectra were realized by a solution of integral equations for intensity and polarization of the coherent spectra [12]. In the energy range of the measurements, the photon beam, polarization ranged from 50% to 70%.

The cross section asymmetry Σ of the reaction $\gamma p \rightarrow \pi^0 p$ is defined as:

$$\Sigma = \frac{1}{P_\gamma} \frac{C_\perp - C_\parallel}{C_\perp + C_\parallel} , \quad (1)$$

where P_γ is the polarization of photon beam and $C_{\perp,\parallel}$ are the normalized yields for the photons polarized perpendicular and parallel to the reaction plane.

The systematic errors of the measurements were dominated mainly by the accuracy of the linear polarization calculations. The uncertainties in $\sigma P_\gamma/P_\gamma$ have been evaluated to be within $\approx 2.3\%$ in full energy range and are included in the errors of the experimental data. The possible shift in the reconstructed photon energies was calculated from the uncertainty in the MS optics and did not exceed 0.4%. Finally, overall systematic uncertainty for each energy set did not exceed 3%.

It is also important to note, that most kinematic bins were formed from at least two independent data samples collected at different kinematic settings of the detector. The final asymmetry was calculated from the corresponding results in such overlapping bins. On the other hand, comparison of the results on such equivalent bins, produced from different event samples, with different acceptance conditions and polarized incident photons from different parts of the CB spectrum, provided a good check for systematic uncertainties in the obtained results.

IV. RESULTS AND DISCUSSION

Our data for the asymmetry Σ , in the kinematic range $E_\gamma = 0.5 - 1.1$ GeV and $\theta_\pi^* = 85^\circ - 125^\circ$, are presented in Table 1. Some of the measured energy and angular distributions are shown in Figs. 7 – 9 together with the experimental data of other groups [13–17] and predictions of different phenomenological analyses [18,19].

The most systematic measurements of Σ for $\gamma p \rightarrow \pi^0 p$, over the resonance region, exist for the angle $\theta_\pi^* = 90^\circ$ (Fig. 7a). From Fig. 7a, one can see, as a whole, a good agreement between the values of prior measurements and our present results. Near 900 MeV, our data disagree with data from MIT [14] and some early SLAC [13] measurements, but are in good agreement with later measurements from another SLAC group [15]. Our points are also consistent with the results of this group for the angle $\theta_\pi^* = 110^\circ$ (Fig. 8b). From Fig. 9, it is seen that our results for the angular distributions at $E_\gamma = 700, 750, \text{ and } 800$ MeV are in agreement with the existing data as well.

In Figs. 7 – 9, the experimental data are also compared with the predictions of phenomenological analyses from the Mainz [18] and GW [19] groups. While both analyses reproduce the qualitative behavior of Σ , a shape discrepancy is noticeable in the GW fit. The main difference between multipole analyses and experiment is observed above $E_\gamma = 700$ MeV where there have been few previous measurements. Inclusion of our data in the GW fit results in an improved description, but shape differences remain. The Mainz fit appears to have a shape more consistent with the data. (It should be noted that some of the older fits, in particular the fit of Ref. [21], predict a shape consistent with the Mainz result.)

It is interesting to compare these results to those recently published by the GRAAL collaboration [6]. In that work, a similar comparison was made for Σ measurements in the reaction $\gamma p \rightarrow \pi^+ n$. There a deviation from GW predictions was noted in the 800

– 1000 MeV range, at backward angles. It was suggested that this discrepancy could be removed by a change in the N(1650) photo-decay amplitude ($A_{1/2}$). We have examined the GRAAL angular distribution at 950 MeV ($W_{CM} = 1630$ MeV) and agree that a change (reduction) in the $E_{0+}^{1/2}$ multipole can account for the shape difference. Here too, for neutral pion production and energies near 900 MeV, a reduction of this multipole in FA00 by about 20% (in modulus) results in an improved description. A reduction of the same amount is found in comparing the energy-dependent and single-energy solutions. The effect is displayed in Fig. 10. Note that this modification to the GW fit, while improving the agreement with data, actually worsens the agreement with the Mainz prediction at the most backward angles.

V. CONCLUSION

The obtained data on cross section asymmetry (Σ) are in good agreement with existing experimental data and in at least qualitative agreement with phenomenological predictions [18,19,21]. We have found evidence in support of the GRAAL claim that some discrepancies with previous GW analyses could be linked to the $E_{0+}^{1/2}$ multipole and possibly the N(1650) resonance contribution. It will be useful to have a Mainz fit including these data in order to isolate differences with the GW fits. A set of fits employing identical data sets would also be useful in determining whether differences are due to the chosen formalism or data constraints. Work along this line is in progress [22].

In summary, results of present experiment on Σ asymmetry have significantly improved the existing data base in the second and third resonance regions. Forthcoming measurements of cross section and polarization observables in the photoproduction of mesons (JLab [20,23], GRAAL [25]), may lead to more successful determinations of the underlying scattering amplitudes and a more precise determination of resonance photocouplings.

ACKNOWLEDGMENTS

The YERPHI group is indebted to the synchrotron staff and cryogenic service for reliable operation during the experiment. This work was supported in part by the Armenian Ministry of Science (Grant-933) and the U. S. Department of Energy Grant DE-FG02-99ER41110. The GW group gratefully acknowledges a contract from Jefferson Lab under which this work was done. Jefferson Lab is operated by the Southeastern Universities Research Association under the U. S. Department of Energy Contract DE-AC05-84ER40150.

REFERENCES

- [1] D. E. Groom *et al.*, Eur. Phys. J. **C15**, 1 (2000).
- [2] R. M. Davidson, N. C. Mukhopadhyay, M. S. Pierce, R. A. Arndt, I. I. Strakovsky, and R. L. Workman, Phys. Rev. C **59**, 1059 (1999).
- [3] L. Tiator, D. Drechsel, G. Knöchlein, and C. Bennhold, Phys. Rev. C **60**, 035210 (1999).
- [4] R. L. Workman, R. A. Arndt, and I. I. Strakovsky, Phys. Rev. C **62**, 048201 (2000).
- [5] T. Mart and C. Bennhold, Phys. Rev. C **61**, 012201 (1999).
- [6] J. Ajaka *et al.*, Phys. Lett. **B475**, 372 (2000).
- [7] A. Vartapetian. Ph.D. Thesis, Hamburg University, 1994;
<http://home.cern.ch/~vartap/phd/phd.ps.gz>
- [8] F. V. Adamian *et al.*, J. Phys. **G19**, L139 (1993).
- [9] F. V. Adamian *et al.*, Preprint YERPHI-1488(5)-97, Yerevan.
- [10] D. Drechsel, O. Hanstein, S. S. Kamalov, and L. Tiator, Nucl. Phys. **A645**, 145 (1999).
- [11] F. V. Adamian *et al.*, J. Phys. **G17**, 1189 (1991).
- [12] H. H. Akopian *et al.*, Preprint YERPHI-908(59)-86, Yerevan;
http://home.cern.ch/~vartap/scanned_preprints/908_86.html
- [13] R. Zdarko and E. Dally, Nuovo Cim. **A10**, 10 (1972).
- [14] J. Alspector *et al.*, Phys. Rev. Lett. **28**, 1403 (1972).
- [15] G. Knies *et al.*, Phys. Rev. D **10**, 2778 (1974).
- [16] V. Ganenko *et al.*, Phys. At. Nucl. (former Sov. J. Nucl. Phys.) **23**, 162 (1976); A. A. Belyaev *et al.*, Nucl. Phys. **B213**, 201 (1983) and references therein.
- [17] R. O. Avakyan *et al.*, Phys. At. Nucl. (former Sov. J. Nucl. Phys.) **40**, 588 (1984) and references therein.
- [18] L. Tiator *et al.*, in preparation.
- [19] R. A. Arndt *et al.*, Phys. Rev. C **53**, 430 (1996); R. A. Arndt *et al.*, in preparation.
- [20] W. J. Briscoe *et al.*, TJNAF/CEBAF experiment proposal E-94-103, 1994.
- [21] I. M. Barbour *et al.*, Nucl. Phys. **B141**, 253 (1978).
- [22] L. Tiator, private communications, 2000.
- [23] D. F. Geesman *et al.*, TJNAF/CEBAF experiment proposal E-94-012, 1994,
D. Jenkins, TJNAF/CEBAF Letter of Intent LOI-96-001, 1996.
- [24] P. J. Bussey *et al.*, Nucl. Phys. **B154**, 205 (1979).
- [25] V. Kouznetsov *et al.*, to be published in Proceedings of IX Moscow International Seminar on Electromagnetic Interactions off Nuclei at Low and Medium Energies, Institute for Nuclear Research, Moscow, Russia, 21-23 Sept. 2000.

TABLES

$\theta^* = 85^\circ \pm 2.5^\circ$			$\theta^* = 90^\circ \pm 2.5^\circ$			$\theta^* = 95^\circ \pm 2.5^\circ$		
E_γ (MeV)	Σ	σ_Σ	E_γ (MeV)	Σ	σ_Σ	E_γ (MeV)	Σ	σ_Σ
500 ± 12.5	0.564	0.081	500 ± 12.5	0.643	0.060	500 ± 12.5	0.643	0.060
525	0.683	0.052	525	0.636	0.039	525	0.617	0.039
550	0.572	0.039	550	0.600	0.031	550	0.636	0.031
575	0.638	0.034	575	0.640	0.028	575	0.627	0.029
600	0.686	0.032	600	0.681	0.027	600	0.693	0.030
625	0.720	0.031	625	0.718	0.027	625	0.715	0.033
650	0.764	0.031	650	0.776	0.028	650	0.702	0.041
675	0.828	0.031	675	0.802	0.030	675	0.756	0.063
700	0.864	0.032	700	0.845	0.035	700	0.878	0.032
725	0.876	0.033	725	0.843	0.025	725	0.864	0.027
750	0.854	0.032	750	0.842	0.025	750	0.823	0.025
775	0.812	0.031	775	0.746	0.022	775	0.711	0.023
800	0.747	0.030	800	0.679	0.021	800	0.640	0.023
825	0.675	0.031	825	0.671	0.021	825	0.601	0.025
850	0.577	0.024	850	0.541	0.022	850	0.497	0.026
875	0.515	0.026	875	0.475	0.024	875	0.394	0.025
900	0.397	0.028	900	0.353	0.025	900	0.304	0.026
925	0.356	0.030	925	0.223	0.023	925	0.144	0.028
950	0.196	0.031	950	0.076	0.024	950	-0.045	0.031
975	0.168	0.032	975	-0.002	0.026	975	-0.108	0.047
1000	0.105	0.034	1000	-0.054	0.028	1000	-0.144	0.084
1025	0.097	0.032	1025	-0.108	0.039			
1050	0.103	0.042	1050	-0.159	0.064			
1075	-0.032	0.061						

TABLE I. *The experimental results on Σ asymmetry of π° photoproduction.*

$\theta^* = 100^\circ \pm 2.5^\circ$			$\theta^* = 105^\circ \pm 2.5^\circ$			$\theta^* = 110^\circ \pm 2.5^\circ$		
E_γ (MeV)	Σ	σ_Σ	E_γ (MeV)	Σ	σ_Σ	E_γ (MeV)	Σ	σ_Σ
700 ± 12.5	0.867	0.029	700 ± 12.5	0.851	0.029	700 ± 12.5	0.803	0.027
725	0.824	0.029	725	0.794	0.027	725	0.778	0.026
750	0.772	0.027	750	0.720	0.024	750	0.708	0.024
775	0.724	0.026	775	0.692	0.024	775	0.649	0.024
800	0.648	0.025	800	0.645	0.023	800	0.587	0.028
825	0.627	0.026	825	0.585	0.025	825	0.478	0.038
850	0.595	0.029	850	0.524	0.032	850	0.360	0.085
875	0.482	0.038	875	0.382	0.052			
900	0.211	0.058	900	0.204	0.089			

TABLE I. *(continued).*

$\theta^* = 115^\circ \pm 2.5^\circ$			$\theta^* = 120^\circ \pm 2.5^\circ$			$\theta^* = 125^\circ \pm 2.5^\circ$		
E_γ (MeV)	Σ	σ_Σ	E_γ (MeV)	Σ	σ_Σ	E_γ (MeV)	Σ	σ_Σ
500 ± 12.5	0.637	0.071	500 ± 12.5	0.717	0.070			
525	0.728	0.049	525	0.677	0.043	525 ± 12.5	0.739	0.051
550	0.750	0.040	550	0.724	0.033	550	0.744	0.034
575	0.792	0.036	575	0.686	0.028	575	0.718	0.028
600	0.742	0.033	600	0.718	0.029	600	0.700	0.027
625	0.744	0.032	625	0.746	0.029	625	0.649	0.032
650	0.770	0.032	650	0.792	0.027	650	0.744	0.052
675	0.862	0.034	675	0.831	0.027	675	0.731	0.034
700	0.809	0.025	700	0.801	0.028	700	0.727	0.027
725	0.795	0.026	725	0.736	0.028	725	0.690	0.026
750	0.723	0.028	750	0.683	0.025	750	0.641	0.024
775	0.664	0.027	775	0.588	0.023	775	0.557	0.024
800	0.594	0.026	800	0.541	0.024	800	0.537	0.030
825	0.498	0.027	825	0.464	0.020	825	0.384	0.024
850	0.439	0.022	850	0.349	0.025	850	0.315	0.022
875	0.329	0.024	875	0.261	0.022	875	0.257	0.019
900	0.171	0.024	900	0.166	0.019	900	0.135	0.018
925	0.017	0.022	925	0.048	0.018	925	0.047	0.020
950	-0.176	0.022	950	-0.110	0.018	950	-0.133	0.021
975	-0.278	0.023	975	-0.272	0.019	975	-0.253	0.032
1000	-0.397	0.023	1000	-0.384	0.025			
1025	-0.494	0.029	1025	-0.444	0.038			
1050	-0.651	0.042	1050	-0.541	0.071			

TABLE I. (*continued*).

Figure captions

Figure 1. Experimental setup. D is the diamond target; K_{1-2} are collimators; SM_{1-2} are sweeping magnets; H_2 is the liquid hydrogen target; Q is the Wilson quantameter; M is the fast monitor; L_{1-2} are quadrupole lenses; PSM and BM are bending magnets; C_{1-2} is the thin converters; Pb is the lead converter; SF_{1-5} , SB , BF_{1-6} , BB_{1-6} , S_{1-4} , V , T are scintillation counters; H_p , H_{xy} are hodoscopes; \check{C} is the Čerenkov counter; $PS - 30$ is the pair spectrometer; MS is the magnetic spectrometer; \check{C}_s is the Čerenkov spectrometer.

Figure 2. Energy spectra of bremsstrahlung on amorphous and crystal targets for different coherent peak (E_γ^{peak}) and electron (E_e) energies: spectrum with amorphous target; coherent spectrum with $E_e = 3 GeV$ and $E_\gamma^{peak} = 600 MeV$; coherent spectrum with $E_e = 3.5 GeV$ and $E_\gamma^{peak} = 900 MeV$.

Figure 3. Results of the test experiment with the point-like target (solid histogram), compared with the Monte Carlo predictions (dashed histogram), for different proton momenta (P_p) and target locations (X_{targ}).

Figure 4. The peak region of the coherent bremsstrahlung (shown with arrows), measured periodically during the experiment, and used to check the peak position. The peak position is in the correct place (a); it is shifted to the side of lower energies (pair spectrometer channels) (b).

Figure 5. Time-of-flight measurements in MS . The arrows indicate the cut positions selecting a proton candidate. The left peak represents events with pion candidate in MS .

Figure 6. Start-stop measurements between two branches.

Figure 7. Energy dependence of π° photoproduction asymmetry Σ at $\theta^* = 90^\circ$ (a) and 120° (b), respectively. Experimental data are from Yerevan, present experiment (filled circles), SLAC [13] (open triangles), MIT [14] (open circles), SLAC [15] (open squares), Kharkov [16] (filled triangles), and Yerevan, previous measurements [17] (filled squares). Solid (dash-dotted) curves give WI00 (FA00) results by GW [19] versus MAID2000 results by the Mainz group [18] (dashed curves).

Figure 8. Energy dependence of π° photoproduction asymmetry Σ at $\theta^* = 100^\circ$ (a) and 110° (b), respectively. Notation is the same as is in Fig. 7.

Figure 9. Angular dependence of π° photoproduction asymmetry Σ at $E_\gamma = 700 MeV$ (a), $E_\gamma = 750 MeV$ (b), and $E_\gamma = 800 MeV$ (c), respectively. Notation is the same as is in Fig. 7.

Figure 10. Angular dependence of π° (a) and π^+ (b) photoproduction asymmetry Σ at $E_\gamma = 950 MeV$. π° data are present measurements. π^+ data are from GRAAL [6] (filled asterisk) and DNPL [24] (open diamond). Plotted are fits

FA00 (dash-dotted), FA00 with a modified $E_{0+}^{1/2}$ multipole (see text) (solid), and the MAID2000 result [18] (dashed).

FIGURES

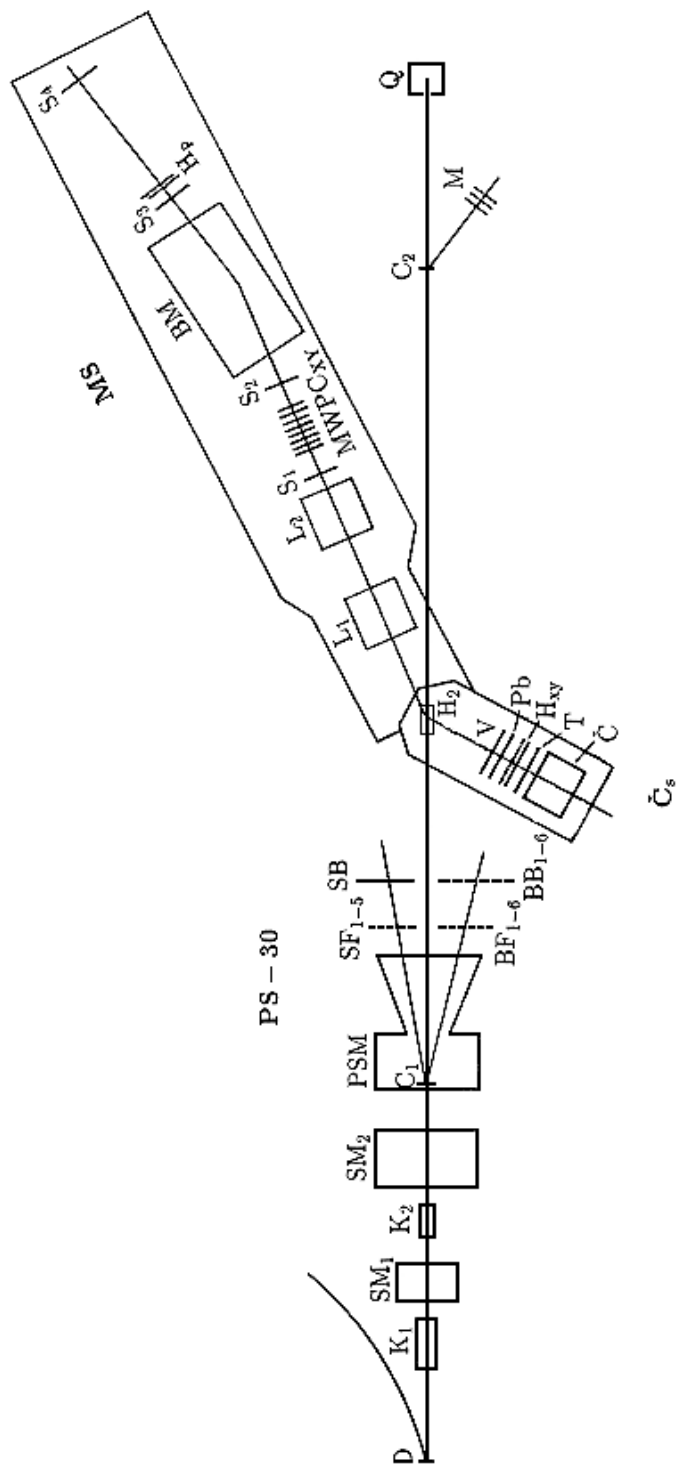


FIG. 1.

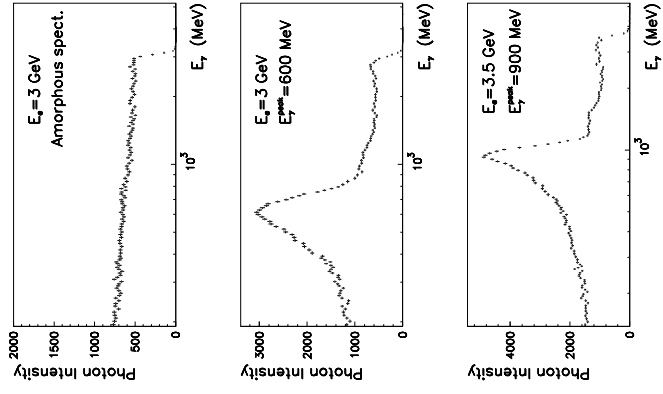


FIG. 2.

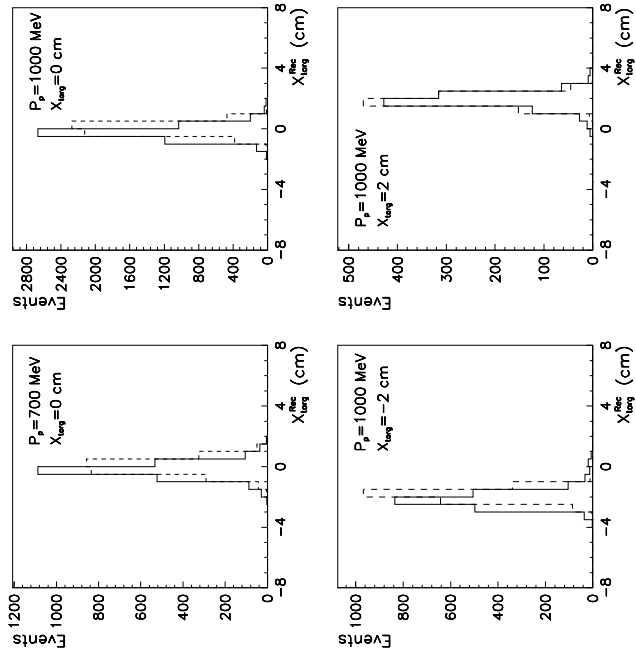


FIG. 3.

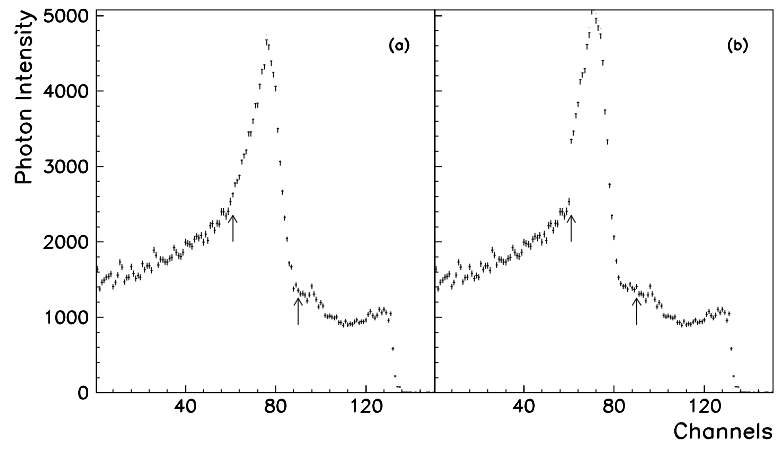


FIG. 4.

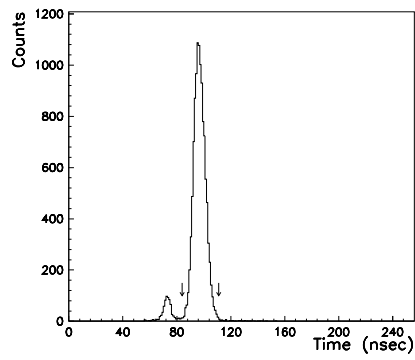


FIG. 5.

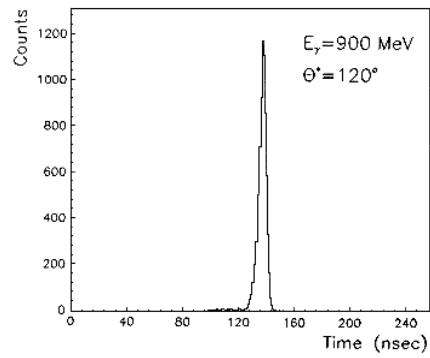


FIG. 6.

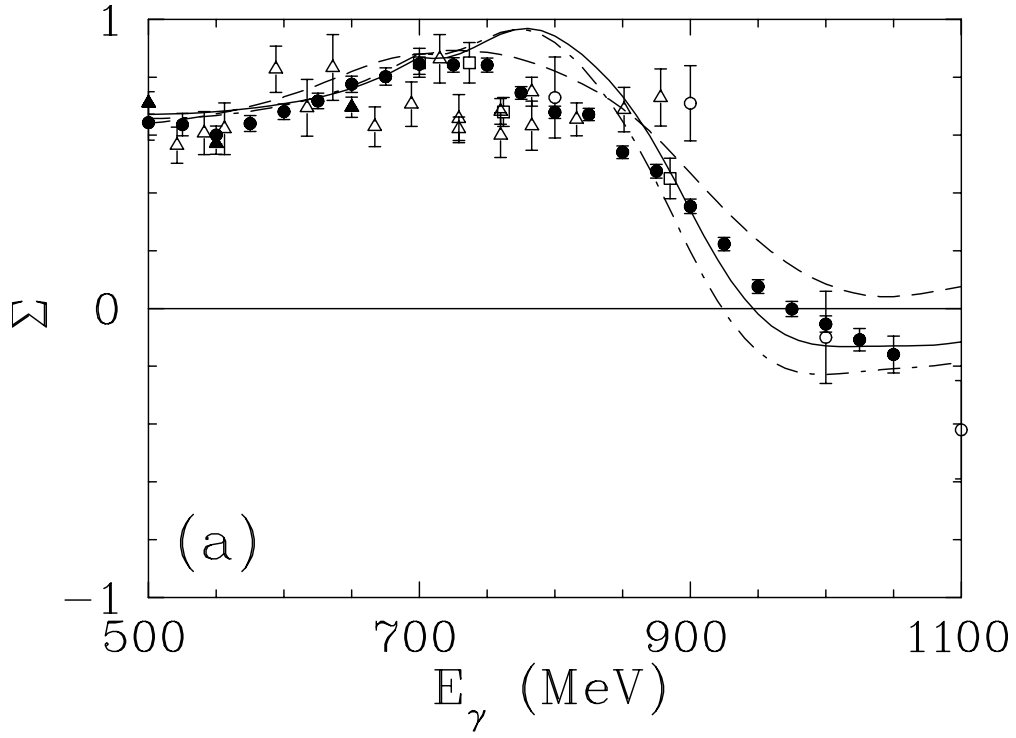


FIG. 7.

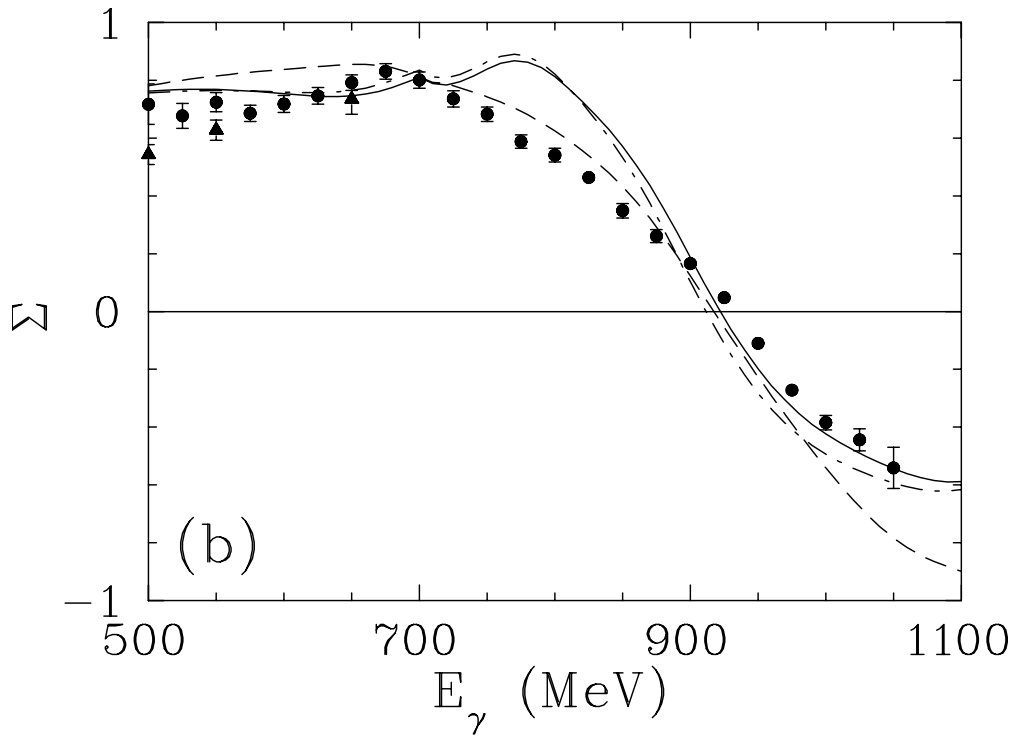


FIG. 8.

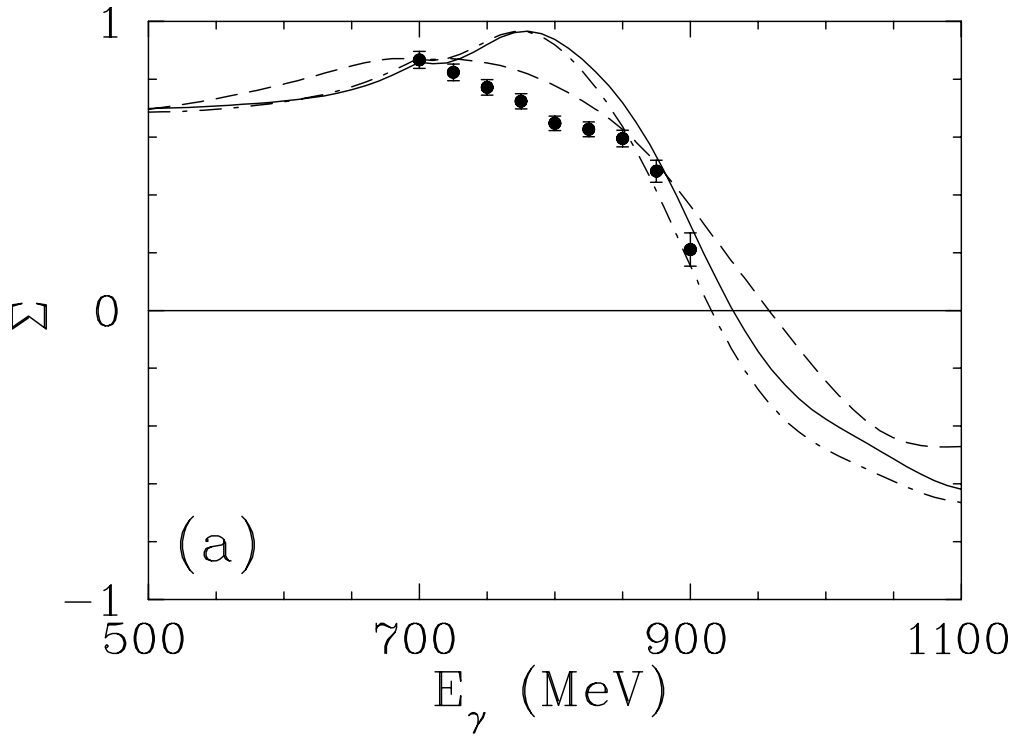


FIG. 9.

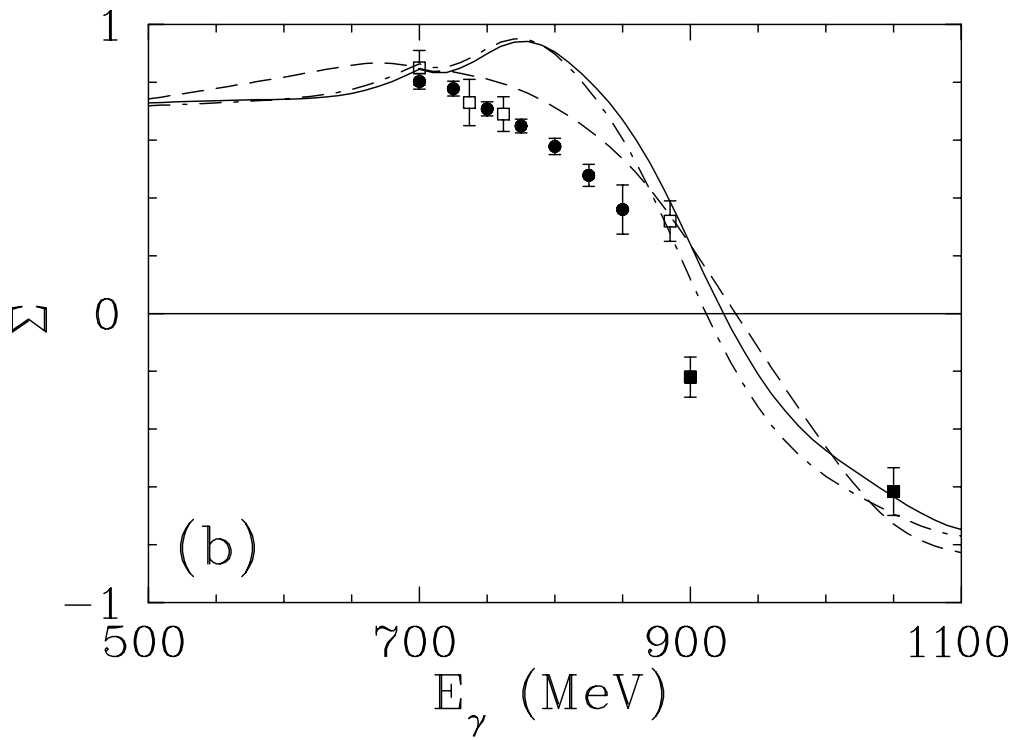


FIG. 10.

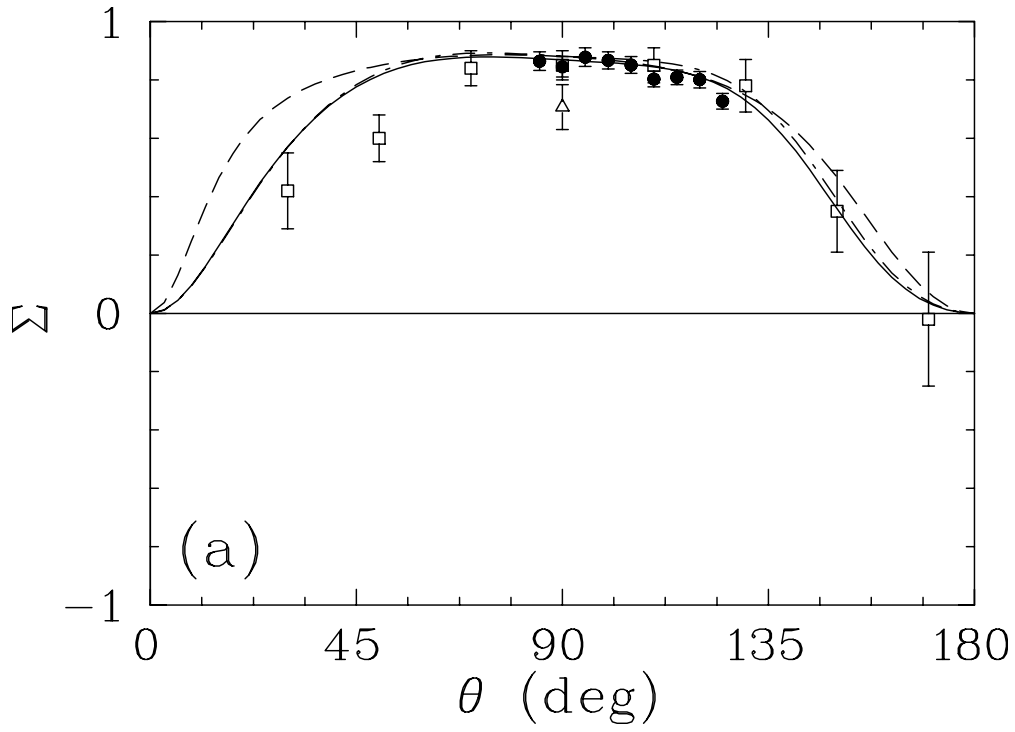


FIG. 11.

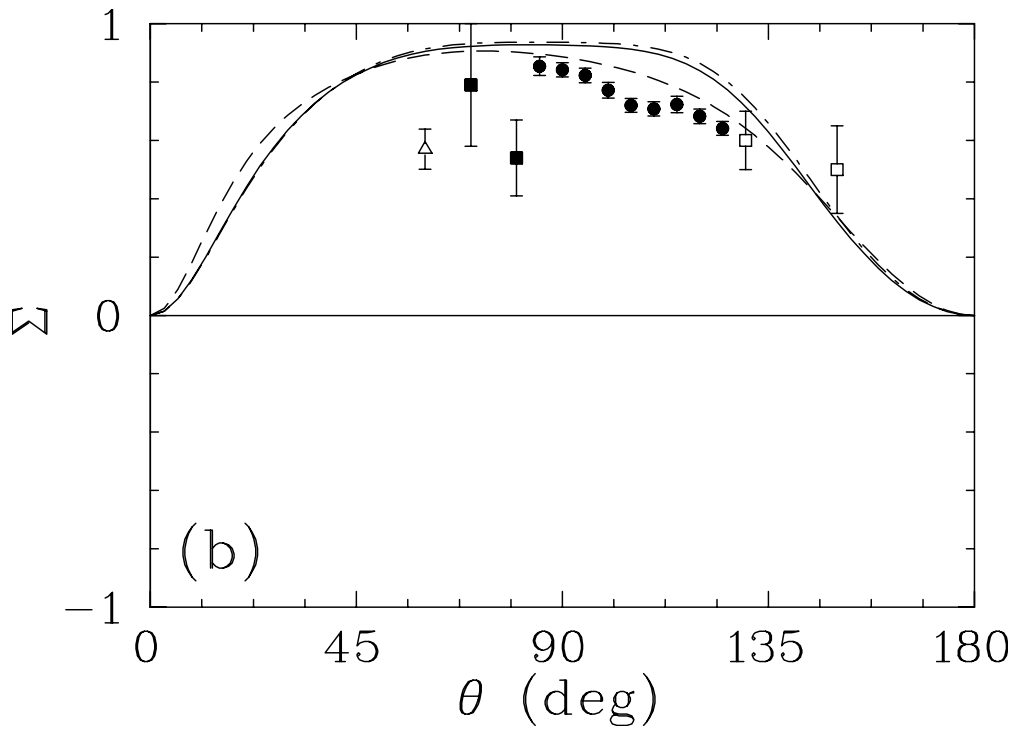


FIG. 12.

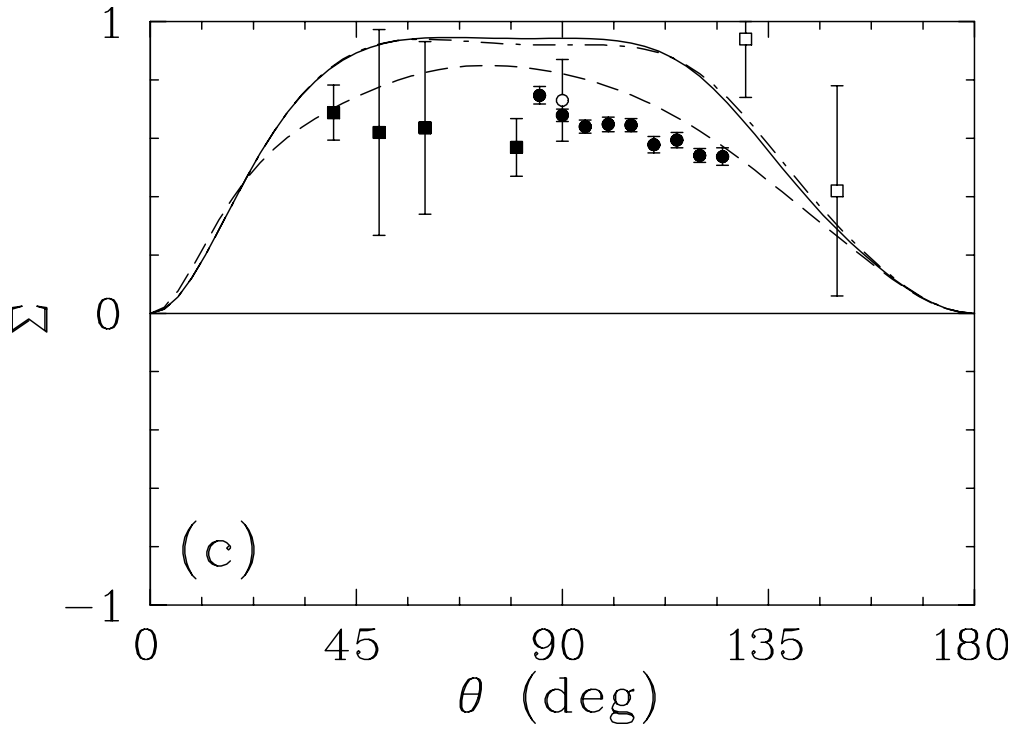


FIG. 13.

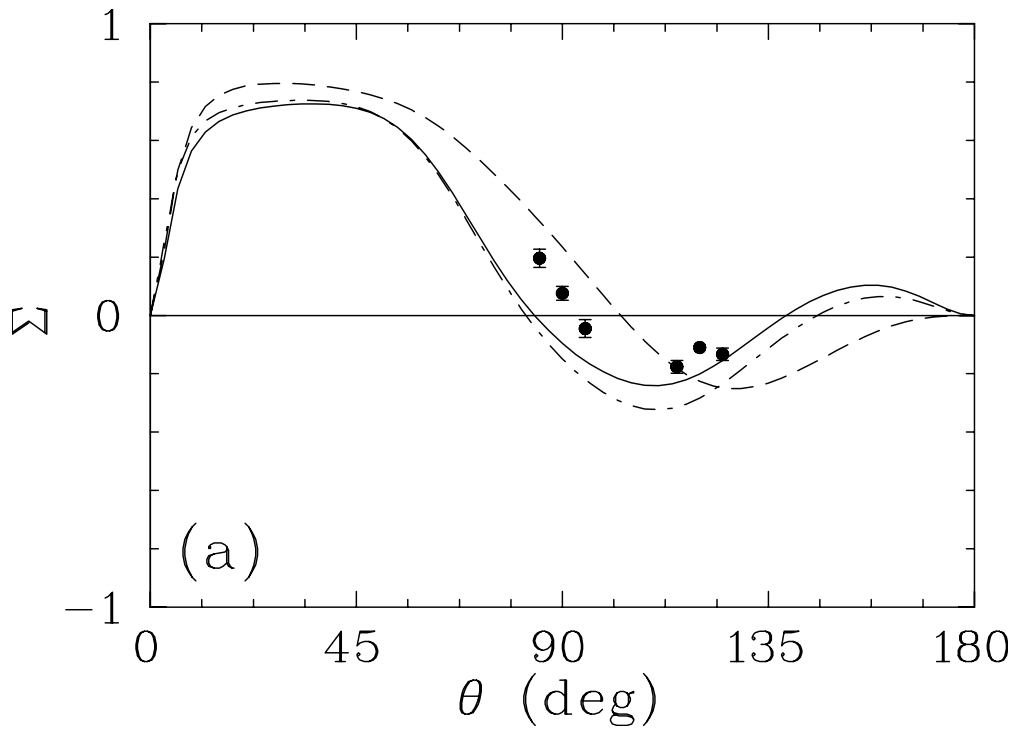


FIG. 14.

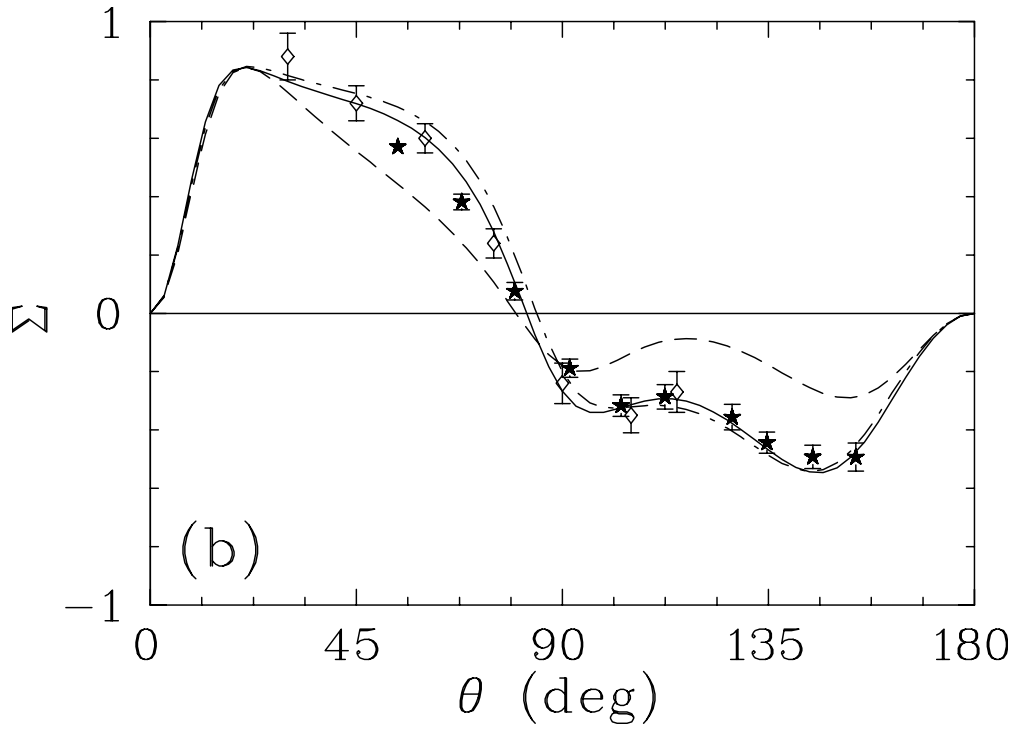


FIG. 15.